Hindawi Publishing Corporation
Advances in Materials Science and Engineering
Volume 2013, Article ID 502702, 6 pages
http://dx.doi.org/10.1155/2013/502702

Research Article

High Pressure Elastic Behavior of Synthetic $Mg_3Y_2(SiO_4)_3$ Garnet up to 9 GPa

Dawei Fan,[1] Maining Ma,[2] Shuyi Wei,[1,3] Zhiqiang Chen,[4] and Hongsen Xie[1]

[1] *Laboratory for High Temperature and High Pressure Study of the Earth's Interior of Institute of Geochemistry, Chinese Academy of Sciences, Guiyang 550002, China*
[2] *Key Laboratory of Computational Geodynamics of Chinese Academy of Sciences, University of Chinese Academy of Sciences, Beijing 100049, China*
[3] *University of Chinese Academy of Sciences, Beijing 100049, China*
[4] *Department of Geosciences, Stony Brook University, Stony Brook, NY 11794, USA*

Correspondence should be addressed to Dawei Fan; fandawei@vip.gyig.ac.cn

Received 5 July 2013; Accepted 14 August 2013

Academic Editor: Pavel Strunz

The compression behavior of synthetic magnesium- (Mg-) yttrium (Y) garnet $Mg_3Y_2(SiO_4)_3$ has been investigated upto about 8.79 GPa at 300 K using *in situ* angle-dispersive X-ray diffraction and a diamond anvil cell at the beamline X17C, National Synchrotron Light Source, Brookhaven National Laboratory. No phase transition has been observed within the pressure range investigated. The unit-cell parameters and volume decreased systematically with increasing pressure, and a reliable isothermal bulk modulus (K_{T0}) and its pressure derivative (K'_{T0}) were obtained in this study. The values of zero-pressure volume V_0, K_0, and K'_0 refined with a third-order Birch-Murnaghan equation of state are $V_0 = 1727.9 \pm 0.2$ Å^3, $K_{T0} = 145 \pm 3$ GPa, and $K'_0 = 8.5 \pm 0.9$. If K'_{T0} is fixed at 4, K_{T0} is obtained as 158 ± 2 GPa.

1. Introduction

Garnets are an important constituent of the upper mantle and mantle transition zone of the Earth and play a fundamental role in high pressure and high temperature petrogenetic processes [1, 2]. Garnets are also important components of subducted oceanic crust, and it is suggested that garnet-rich subducted crust can be gravitationally trapped in the lowermost part of the mantle transition zone [3–6]. Therefore, accurate knowledge of the physical properties of garnets is essential to infer appropriate compositional models for the upper mantle and mantle transition zone of the Earth. In addition, garnet is the major host of the rare-earth element (REE) both in metamorphic rocks and mantle rocks, and the latter may undergo partial melting in the mantle [7]. Thus, there is a considerable interest in the study of the thermodynamic behavior of REE in garnet that could help to understand the evolution of REE patterns in magmas and in the residual solids [7–9], especially garnets in igneous and metamorphic rocks.

Garnets have the general formula $X_3Y_2(SiO_4)_3$, centered cubic lattice (space group *Ia–3d*), and display 8-fold dodecahedral (X), 6-fold octahedral (Y), and tetrahedral (Si) crystallographic sites. This unique behavior makes the garnet structure flexible in accommodating various chemical substitutions with different ionic radii, suggesting that garnets could be composition diverse where X = Mg^{2+}, Fe^{2+}, Ca^{2+}, Mn^{2+}, Y^{3+}; Y = Al^{3+}, Fe^{3+}, Cr^{3+}, and Y^{3+}. Chemical substitutions at octahedral and triangular dodecahedral sites may change the relative bond lengths/interatomic distances and angles, which will result in affecting their elastic properties [6].

Yttrium is a silvery-metallic transition metal chemically similar to the lanthanides, and it has often been classified as a "rare earth element". Yttrium is almost always found combined with the lanthanides in rare-earth minerals [10, 11]. It is used in the production of a large variety of synthetic garnets [12], and yttria is used to make yttrium iron garnets ($Y_3Fe_5O_{12}$, YIG), which are very effective microwave filters.

YIG is also very efficient as an acoustic energy transmitter and transducer [13]. Yttrium aluminium garnet ($Y_3Al_5O_{12}$, YAG) is used in a number of industrial applications, either in the pure phase form or as a composite [14].

To date, the elastic properties of pyrope have been studied extensively by multianvil apparatus and diamond anvil cell [6, 15–22]. However, nowadays, there are no studies available on the elastic behavior of rare-earth silicate garnet at high pressure. In addition, yttrium not only can substitute for Mg at the dodecahedral site but also can substitute for Al at the octahedral site in the silicate garnet. In this paper, we report the elastic measurements of magnesium- (Mg-) yttrium (Y) garnet [$Mg_3Y_2(SiO_4)_3$], a synthetic rare-earth silicate garnet, up to pressures of 8.79 GPa at room temperature. Along with the previous results for pyrope [6, 15–22], the compositional dependence of the bulk modulus is discussed.

2. Sample and Experiment

The $Mg_3Y_2(SiO_4)_3$ sample used in our high pressure powder X-ray diffraction experiments was synthesized with a multianvil pressure apparatus (YJ-3000T) installed at the Institute of Geochemistry, Chinese Academy of Sciences. Details about the apparatus have been described by Xie et al. [23]. The pressurization system of this press consists of six WC anvils, with their tips truncated as $23.5 \times 23.5\,mm^2$, which are simultaneously pushed by six hydraulic rams so that high pressure is generated in the experimental assembly. The experimental assembly, YJ-3000T, used in this study, is schematically illustrated in Figure 1. The experimental temperature was measured and controlled with a $Pt_{94}Rh_6$-$Pt_{70}Rh_{30}$ thermocouple (type B). The starting materials used in the synthesizing experiments were stoichiometric amounts of high purity $MgCO_3$, Y_2O_3, and SiO_2 and were placed one night at 800°C for removing carbonates. The mixture was then melted at 1400°C which produced, after quenching, a homogeneous glass. The homogeneous glass was crushed into a fine powder using acetone. The starting mixtures were encapsulated in platinum capsules. The synthesizing pressure and temperature conditions were 4 GPa and 1000°C for 24 h. The crystal structure of sample was confirmed by using powder X-ray diffraction method (X'Pert Pro MPD system). Their compositions were confirmed by using electron microprobe analysis (EPMA-1600).

In this investigation, we conducted *in situ* high-pressure angle dispersive X-ray diffraction experiments at the beamline X17C, National Synchrotron Light Source (NSLS), Brookhaven National Laboratory, using a 0.37677 Å X-ray beam and CCD detector, and the beamline 4W2, Beijing Synchrotron Radiation Facility (BSRF), using a 0.6199 Å X-ray beam and Mar345 detector. We generated the high pressure by using a symmetrical diamond-anvil cell, equipped with two diamonds anvils (culet face diameter: 500 μm) and tungsten-carbide supports. In these high pressure experiments, T301 stainless steel plates with an initial thickness of 200 μm were used as gaskets, with their central part preindented to a thickness of about 50 μm and then drilled through into a hole of 200 μm diameter. The finely ground

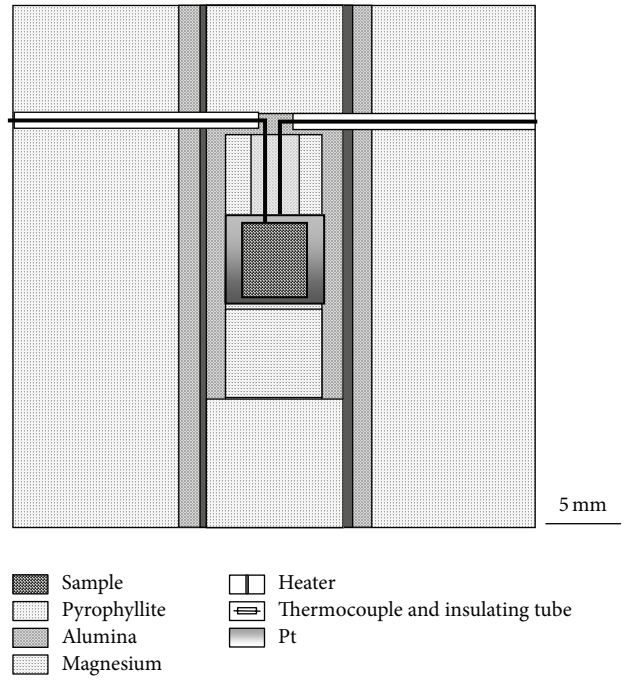

Figure 1: Experimental assembly used in the high pressure synthesizing experiments with a multianvil pressure apparatus (YJ-3000T) installed at the Institute of Geochemistry, Chinese Academy of Sciences.

$Mg_3Y_2(SiO_4)_3$ powder, plus a couple of tiny ruby balls together with a methanol : ethanol : water mixture (16 : 3 : 1 by volume) which is a hydrostatic pressure-transmitting medium up to about 10 GPa [24], was loaded into the gasket hole. The ruby fluorescence method [25] was employed to determine the experimental pressure. The X-ray diffraction patterns (collecting time = 10 min) were integrated to generate the conventional one-dimensional profiles using the Fit2D program [26]. The sample was equilibrated for about 10 min before diffraction data measurement, and subsequently the pressure was raised up to 8.79 GPa. Unit-cell parameters were refined by Le Bail fitting using the GSAS package [27, 28] and user interface EXPGUI [29] up to 8.79 GPa (Table 2). Background was fitted using the Chebyschev polynomial, and X-ray peak shapes were fitted using the pseudo-Voigt profile function proposed by Thomson et al. [30].

3. Result and Discussion

The powder X-ray diffraction data of $Mg_3Y_2(SiO_4)_3$ at ambient conditions revealed that this phase has a cubic structure (*Ia–3d*), with unit-cell dimensions of $a = 11.9995(4)$ Å. The observed and calculated X-ray diffraction patterns of $Mg_3Y_2(SiO_4)_3$ at ambient conditions are listed in Table 1. The volume of $Mg_3Y_2(SiO_4)_3$ unit cell at ambient conditions is $1727.8(2)\,Å^3$.

The high pressure X-ray diffraction data were collected up to 8.79 GPa at ambient temperature. Typical X-ray diffraction spectrums at selected pressure is shown in Figure 2. The diffraction patterns at each pressure of the study are

Table 1: Observed and calculated X-ray diffraction patterns of $Mg_3Y_2(SiO_4)_3$ at ambient conditions.

$h\,k\,l$	d_{obs} (Å)	d_{cal} (Å)	$d_{obs}/d_{cal} - 1$
2 2 0	4.24142	4.24233	−0.00021
3 2 1	3.20735	3.20690	0.00014
4 0 0	2.99925	2.99978	−0.00018
4 2 0	2.68323	2.68308	0.00006
4 2 2	2.44947	2.44931	0.00007
4 3 1	2.35309	2.35322	−0.00006
5 2 1	2.19082	2.19073	0.00004
4 4 0	2.12145	2.12116	0.00014
6 1 1	1.94676	1.94651	0.00013
4 4 4	1.73204	1.73192	0.00007
6 4 0	1.66432	1.66398	0.00020
5 5 2	1.63324	1.63287	0.00023
6 4 2	1.60366	1.60345	0.00013
8 0 0	1.50014	1.49989	0.00017

Calculated d-spacings are based on the cubic unit-cell dimensions of a = 11.9995 Å.

Table 2: Cell parameters versus pressure for $Mg_3Y_2(SiO_4)_3$.

P (GPa)	a (Å)	V (Å^3)
0.0001	11.9995 (4)	1727.8 (2)
0.70	11.9810 (8)	1719.8 (4)
1.69	11.9568 (9)	1709.0 (4)
2.62	11.9325 (9)	1699.0 (4)
3.44	11.9128 (8)	1690.6 (3)
5.14	11.8741 (9)	1674.2 (4)
6.84	11.8399 (9)	1659.7 (4)
7.97	11.8204 (9)	1651.6 (5)
8.79	11.8034 (9)	1644.4 (5)

Numbers in brackets are 1σ error in last digits.

similar to one another up to 8.79 GPa, with Bragg peaks shifted to higher than 2θ. No phase transition occurs within the pressure range investigated. Previous experiments have shown that some of the rare-earth garnets become amorphous at high pressure and room temperature, $Gd_3Ga_5O_{12}$, $Gd_3Sc_2Ga_3O_{12}$, and $Y_3Fe_5O_{12}$ become amorphous at 84, 58, and 50 GPa, [31] respectively, whereas $Mg_3Y_2(SiO_4)_3$ in this study remains crystalline cubic up to 9 GPa. In addition, the garnets may transfer to perovskite phase at high pressure and high temperature [32]. And for the rare-earth garnets, the amorphous-to-perovskite phase transition requires a very high pressure (~80 GPa) and high temperature (~2000 K) [32, 33]. So, laser heating combined with diamond anvil cell is needed in the amorphous-to-perovskite phase transition study of $Mg_3Y_2(SiO_4)_3$ for further research.

The effect of pressure on the unit-cell parameters and volume of $Mg_3Y_2(SiO_4)_3$ are shown in Table 2.

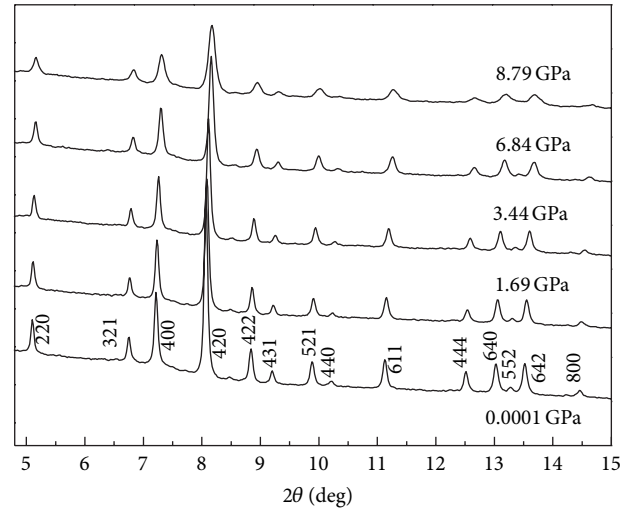

Figure 2: Representative X-ray diffraction patterns of $Mg_3Y_2(SiO_4)_3$ up to 8.79 GPa.

The pressure-volume data have been fitted to the third-order Birch-Murnaghan equation of state (III-BM-EoS) [34] to determine the elastic parameters

$$P = \left(\frac{3}{2}\right) K_{T0} \left[\left(\frac{V_0}{V}\right)^{7/3} - \left(\frac{V_0}{V}\right)^{5/3}\right] \times \left\{1 + \left(\frac{3}{4}\right)\left(K'_{T0} - 4\right)\left[\left(\frac{V_0}{V}\right)^{2/3} - 1\right]\right\}, \quad (1)$$

where V_0, V, K_{T0}, and K'_{T0} are the zero-pressure volume, high-pressure volume, isothermal bulk modulus, and its pressure derivative, respectively. The results from a least-squares fitting using an EosFit program [35] are V_0 = 1727.9(2) Å^3, K_{T0} = 145(3) GPa, and K'_{T0} = 8.5(9), respectively. When K'_{T0} is set as 4, the isothermal bulk modulus is determined as 158(2) GPa. The unit-cell volume data as a function of pressure and the compression curve calculated from these fitted parameters are plotted in Figure 3.

To assess the quality of the Birch-Murnaghan equation of state fit obtained from the plot of unit-cell volume against pressure, the relationship between the Eulerian strain ($f_E = 0.5[(V_0/V)^{2/3} - 1]$) and the normalized pressure ($F_E = P/[3f_E(2f_E + 1)^{5/2}]$) was plotted [35], and it is shown in Figure 4. The F_E-f_E plot provides a visual indication of which higher order terms, such as K'_{T0}, are significant in the equation of state. The $Mg_3Y_2(SiO_4)_3$ data showed a relatively large positive slope (Figure 4). This indicates that the pressure derivative of the bulk modulus (K'_{T0}) was larger than 4. Therefore, the value, estimated to be 8.5(9), was consistent with the F_E-f_E plot analysis.

Table 3 and Figure 3 show a comparison of this study and the previous studies for pyrope at room temperature. So far, the elasticity of pyrope has been studied intensively [6, 15–22], and various reports on K_{T0} of pyrope converge to K_{T0} = 167–175 GPa. The K_{T0} value of 145(3) GPa obtained in this study for $Mg_3Y_2(SiO_4)_3$ is about 15% smaller than

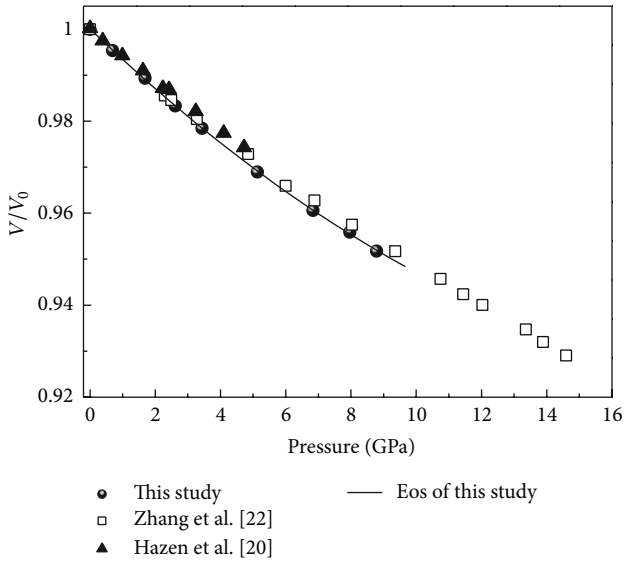

Figure 3: Volume compression of synthetic $Mg_3Y_2(SiO_4)_3$ at high pressure and room temperature.

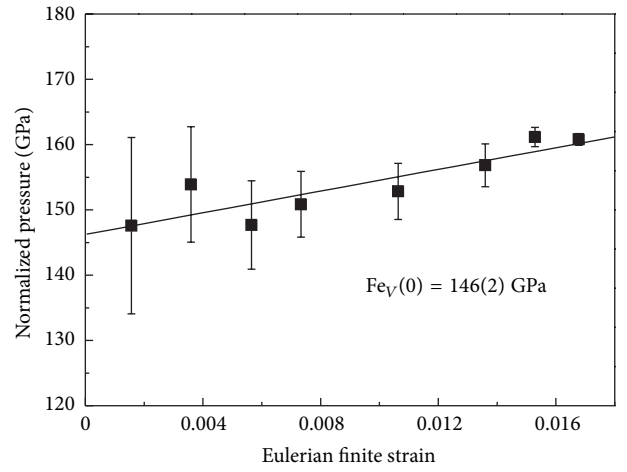

Figure 4: Eulerian strain-normalized pressure (f_E-F_E) plot of the data based on the Birch-Murnaghan equation of state. The solid line represents the linear fit.

the values of pyrope. However, the parameters K_{T0} and K'_{T0} are usually strongly correlated in an EoSfit [36], so we cannot just compare the bulk modulus and neglect its pressure derivative. Therefore, we compared the results of this study with Hazen et al. and Zou et al. by fixing K'_{T0} to 4.0. From Table 3, we can find that the bulk moduli of Hazen et al. [20] and Zou et al. [6] by fixing K'_{T0} to 4.0 are 174(3) and 171(1) GPa, respectively. The K_{T0} value of 158(2) GPa obtained in this study for $Mg_3Y_2(SiO_4)_3$ by fixing K'_{T0} to 4.0 is still about 10% smaller than the values of pyrope by fixing K'_{T0} to 4.0. There are two possible sources for K_{T0} of this study for $Mg_3Y_2(SiO_4)_3$ smaller than the results of pyrope for $Mg_3Al_2(SiO_4)_3$. First, the ionic radius of Al and Y is increasing [Al^{3+} (0.51 Å) < Y^{3+} (0.89 Å)]. Fan et al. [37] studied the grossular-andradite solid solution

Table 3: Elastic parameters derived from the Birch-Murnaghan EoS of $Mg_3Y_2(SiO_4)_3$ garnet, as compared with previous studies of pyrope garnet.

Sample	K_0 (GPa)	K'_0	Reference
Pyrope			
	171 (3)	1.8 (7)	Sato et al. (1978) [15]
	175 (1)	4.5 (5)	Levien et al. (1979) [17]
	172.8[a]	3.8 (1.0)	Leger et al. (1990) [18]
	174 (3)	4.0[a]	Hazen et al. (1994) [20]
	171 (2)	4.4 (2)	Zhang et al. (1998) [22]
	167 (6)	4.6 (3)	Zou et al. (2012) [6]
	171 (1)	4.0[a]	Zou et al. (2012) [6]
$Mg_3Y_2(SiO_4)_3$	145 (3)	8.5 (9)	This study
	158 (2)	4.0[a]	This study

[a]Fixed at this value during data processing.
Numbers in brackets are 1σ error in last digits.

using high pressure X-ray diffraction and showed the bulk modulus of grossular-andradite solid solution decreases with the increasing andradite content. They considered that the ionic radii of Al^{3+} (0.51 Å) smaller than those of Fe^{3+} (0.64 Å) had a significant influence on bulk modulus of grossular-andradite solid solution. In addition, Liu et al. [38] also suggested that the differences in the elastic behavior of lead fluorapatite and calcium apatites were attributed to the different ionic sizes of Pb^{2+} (1.19 Å) and Ca^{2+} (1.00 Å). Second, we consider that the electronegativity number may be another factor for this situation (1.61 for Al compared with 1.22 for Y). Electronegativity is a chemical property that describes the ability of an atom to attract electrons [39, 40]. An atom's electronegativity is affected by its atomic weight and the distance of its valence electrons from the charged nucleus [39, 41]. The higher the associated electronegativity number is, the greater an element or compound attracts electrons [41]. The electronegativity is larger, the attraction for bonding electron is stronger, and the electron density between cation and anion is greater, resulting in the fact that crystals have greater compressed resisted capacity [42, 43]. The ionic radius and electronegativity may be having a significant influence on bulk modulus [41, 44]. The smaller of ionic radius and larger electronegativity, the stronger of attraction for bonding electron, the greater of electron density between cation and anion, resulting in crystals have greater compressed resisted capacity [41, 44]. Therefore, we infer that the ionic radius and electronegativity is the main reason for the bulk moduli of this study smaller than the values of pyrope.

4. Conclusion

The *P-V* measurements on a synthetic $Mg_3Y_2(SiO_4)_3$ at pressures up to 8.79 GPa were carried out using angle-dispersive X-ray diffraction technique. No phase transition has been observed within the pressure range investigated. The *P-V* equation of state for the $Mg_3Y_2(SiO_4)_3$, fitted using the third-order Birch-Murnaghan equation of state, gives

$V_0 = 1727.9 \pm 0.2$ Å^3, $K_{T0} = 145 \pm 3$ GPa, and $K'_{T0} = 8.5 \pm 0.9$. The value of the bulk modulus in this study for $Mg_3Y_2(SiO_4)_3$ is smaller than that of pyrope reported previously, which can be attributed to the different ionic radii and electronegativity.

Acknowledgments

This work is supported by the National Natural Science Foundation of China (Grant nos. 41374107, 41004035, and 41274105) and the Western Doctor Special Fund of the West Light Foundation of the Chinese Academy of Sciences (2011, to Fan Dawei). Use of the National Synchrotron Light Source, Brookhaven National Laboratory, was supported by the U.S. Department of Energy, Office of Science, Office of Basic Energy Sciences, under Contract no. DE-AC02-98CH10886. The 4W2 High Pressure Station, Beijing Synchrotron Radiation Facility (BSRF), is supported by the Chinese Academy of Sciences (Grant nos. KJCX2-SW-N20, KJCX2-SW-N03).

References

[1] T. Irifune and A. E. Ringwood, "Phase transformations in a harzburgite composition to 26 GPa: implications for dynamical behaviour of the subducting slab," *Earth and Planetary Science Letters*, vol. 86, no. 2–4, pp. 365–376, 1987.

[2] A. Pavese, D. Levy, and V. Pischedda, "Elastic properties of andradite and grossular, by synchrotron X-ray diffraction at high pressure conditions," *European Journal of Mineralogy*, vol. 13, no. 5, pp. 929–937, 2001.

[3] T. Irifune and A. E. Ringwood, "Phase transformations in subducted oceanic crust and buoyancy relationships at depths of 600–800 km in the mantle," *Earth and Planetary Science Letters*, vol. 117, no. 1-2, pp. 101–110, 1993.

[4] S.-I. Karato, Z. Wang, B. Liu, and K. Fujino, "Plastic deformation of garnets: systematics and implications for the rheology of the mantle transition zone," *Earth and Planetary Science Letters*, vol. 130, no. 1–4, pp. 13–30, 1995.

[5] S. Gréaux, Y. Kono, N. Nishiyama, T. Kunimoto, K. Wada, and T. Irifune, "P-V-T equation of state of $Ca_3Al_2Si_3O_{12}$ grossular garnet," *Physics and Chemistry of Minerals*, vol. 38, no. 2, pp. 85–94, 2011.

[6] Y. T. Zou, S. Greaux, T. Irifune, M. L. Whitaker, T. Shinmei, and Y. Higo, "Thermal equation of state of $Mg_3Al_2Si_3O_{12}$ pyrope garnet up to 19 GPa and 1700 K," *Physics and Chemistry of Minerals*, vol. 39, no. 7, pp. 589–598, 2012.

[7] M. Tirone, J. Ganguly, R. Dohmen, F. Langenhorst, R. Hervig, and H.-W. Becker, "Rare earth diffusion kinetics in garnet: experimental studies and applications," *Geochimica et Cosmochimica Acta*, vol. 69, no. 9, pp. 2385–2398, 2005.

[8] M. Tirone, *Diffusion of rare earth elements in garnet and pyroxene: experiment, theory and applications [Ph.D. thesis]*, University of Arizona, 2002.

[9] D. D. Hickmott, "Rare earth element zoning in pyrope-rich garnet from mantle xenoliths," *Annual Report of the Director of the Geo-Physical Laboratory*, vol. 1988-1989, pp. 6–10, 1989.

[10] P. Roychowdhury, N. K. Roy, D. K. Das, and A. K. Das, "Determination of rare-earth elements and yttrium in silicate rocks by sequential inductively-coupled plasma emission spectrometry," *Talanta*, vol. 36, no. 12, pp. 1183–1186, 1989.

[11] N. Planavsky, A. Bekker, O. J. Rouxel et al., "Rare Earth Element and yttrium compositions of Archean and Paleoproterozoic Fe formations revisited: new perspectives on the significance and mechanisms of deposition," *Geochimica et Cosmochimica Acta*, vol. 74, no. 22, pp. 6387–6405, 2010.

[12] H. W. Jaffe, "The role of yttrium and other minor elements in the garnet group," *American Mineralogist*, vol. 36, pp. 133–155, 1951.

[13] S. Hosseini Vajargah, H. R. Madaah Hosseini, and Z. A. Nemati, "Preparation and characterization of yttrium iron garnet (YIG) nanocrystalline powders by auto-combustion of nitrate-citrate gel," *Journal of Alloys and Compounds*, vol. 430, no. 1-2, pp. 339–343, 2007.

[14] X. Z. Guo, P. S. Devi, B. G. Ravi, J. B. Parise, S. Sampath, and J. C. Hanson, "Phase evolution of yttrium aluminium garnet (YAG) in a citrate-nitrate gel combustion process," *Journal of Materials Chemistry*, vol. 14, no. 8, pp. 1288–1292, 2004.

[15] Y. Sato, M. Akaogi, and S. Akimoto, "Hydrostatic compression of the synthetic garnets pyrope and almandine," *Journal of Geophysical Research*, vol. 83, no. 1, pp. 335–338, 1978.

[16] R. M. Hazen and L. W. Finger, "Crystal structures and compressibilities of pyrope and grossular to 60 kbar," *American Mineralogist*, vol. 63, no. 3-4, pp. 297–303, 1978.

[17] L. Levien, C. T. Prewitt, and D. J. Weidner, "Compression of pyrope," *American Mineralogist*, vol. 64, no. 7-8, pp. 805–808, 1979.

[18] J. M. Leger, A. M. Redon, and C. Chateau, "Compressions of synthetic pyrope, spessartine and uvarovite garnets up to 25 GPa," *Physics and Chemistry of Minerals*, vol. 17, no. 2, pp. 161–167, 1990.

[19] R. M. Hazen and L. W. Finger, "High-pressure crystal chemistry of andradite and pyrope: revised procedures for high-pressure diffraction experiments," *American Mineralogist*, vol. 74, no. 3-4, pp. 352–359, 1989.

[20] R. M. Hazen, R. T. Downs, P. G. Conrad, L. W. Finger, and T. Gasparik, "Comparative compressibilities of majorite-type garnets," *Physics & Chemistry of Minerals*, vol. 21, no. 5, pp. 344–349, 1994.

[21] Y. Wang, D. J. Weidner, J. Zhang, G. D. Gwanrnesia, and R. C. Liebermann, "Thermal equation of state of garnets along the pyrope-majorite join," *Physics of the Earth and Planetary Interiors*, vol. 105, no. 1-2, pp. 59–71, 1998.

[22] L. Zhang, H. Ahsbahs, and A. Kutoglu, "Hydrostatic compression and crystal structure of pyrope to 33 GPa," *Physics and Chemistry of Minerals*, vol. 25, no. 4, pp. 301–307, 1998.

[23] H.-S. Xie, Y.-M. Zhang, H.-G. Xu, W. Hou, J. Guo, and H.-R. Zhao, "A new method of measurement for elastic wave velocities in minerals and rocks at high temperature and high pressure and its significance," *Science in China B*, vol. 36, no. 10, pp. 1276–1280, 1993.

[24] R. J. Angel, M. Bujak, J. Zhao, G. D. Gatta, and S. D. Jacobsen, "Effective hydrostatic limits of pressure media for high-pressure crystallographic studies," *Journal of Applied Crystallography*, vol. 40, no. 1, pp. 26–32, 2007.

[25] H. K. Mao, P. M. Bell, J. W. Shaner, and D. J. Steinberg, "Specific volume measurements of Cu, Mo, Pd, and Ag and calibration of the ruby R1 fluorescence pressure gauge from 0.06 to 1 Mbar," *Journal of Applied Physics*, vol. 49, no. 6, pp. 3276–3283, 1978.

[26] J. Hammersley, *Fit2D Report*, European Synchrotron Radiation Facility, Grenoble, France, 1996.

[27] A. C. Larson and R. B. von Dreele, "General Structure Analysis System (GSAS) operation manual," Report, Los Alamos National Laboratory, 2000.

[28] A. Le Bail, H. Duroy, and J. L. Fourquet, "Ab-initio structure determination of $LiSbWO_6$ by X-ray powder diffraction," *Materials Research Bulletin*, vol. 23, no. 3, pp. 447–452, 1988.

[29] B. H. Toby, "EXPGUI, a graphical user interface for GSAS," *Journal of Applied Crystallography*, vol. 34, no. 2, pp. 210–213, 2001.

[30] P. Thomson, D. E. Cox, and J. B. Hastings, "Rietveld refinement of Debye-Scherrer synchrotron X-ray data from Al_2O_3," *Journal of Applied Crystallography*, vol. 20, no. 2, pp. 79–83, 1987.

[31] H. Hua, S. Mirov, and Y. K. Vohra, "High-pressure and high-temperature studies on oxide garnets," *Physical Review B*, vol. 54, no. 9, pp. 6200–6209, 1996.

[32] C. L. Lin, J. Liu, J. F. Lin et al., "Garnet-to-Perovskite transition in $Gd_3Sc_2Ga_3O_{12}$ at high pressure and high temperature," *Inorganic Chemistry*, vol. 52, no. 1, pp. 431–434, 2013.

[33] Z. Mao, S. M. Dorfman, S. R. Shieh et al., "Equation of state of a high-pressure phase of $Gd_3Ga_5O_{12}$," *Physical Review B*, vol. 83, no. 5, Article ID 054114, 2011.

[34] F. Birch, "Finite elastic strain of cubic crystals," *Physical Review*, vol. 71, no. 11, pp. 809–824, 1947.

[35] R. J. Angel, "Equation of state," *Reviews in Mineralogy and Geochemistry*, vol. 41, no. 1, pp. 35–60, 2001.

[36] K. K. M. Lee, B. O'Neill, W. R. Panero, S.-H. Shim, L. R. Benedetti, and R. Jeanloz, "Equations of state of the high-pressure phases of a natural peridotite and implications for the Earth's lower mantle," *Earth and Planetary Science Letters*, vol. 223, no. 3-4, pp. 381–393, 2004.

[37] D.-W. Fan, S.-Y. Wei, J. Liu, Y.-C. Li, and H.-S. Xie, "High pressure X-ray diffraction study of a grossular-andradite solid solution and the bulk modulus variation along this solid solution," *Chinese Physics Letters*, vol. 28, no. 7, Article ID 076101, 2011.

[38] X. Liu, S. R. Shieh, M. E. Fleet, and A. Akhmetov, "High-pressure study on lead fluorapatite," *American Mineralogist*, vol. 93, no. 10, pp. 1581–1584, 2008.

[39] L. C. Allen, "Electronegativity is the average one-electron energy of the valence-shell electrons in ground-state free atoms," *Journal of the American Chemical Society*, vol. 111, no. 25, pp. 9003–9014, 1989.

[40] R. P. Iczkowski and J. L. Margrave, "Electronegativity," *Journal of the American Chemical Society*, vol. 83, no. 17, pp. 3547–3551, 1961.

[41] J. Zhang, "Room-temperature compressibilities of MnO and CdO: further examination of the role of cation type in bulk modulus systematics," *Physics and Chemistry of Minerals*, vol. 26, no. 8, pp. 644–648, 1999.

[42] C. Li, Y. L. Chin, and P. Wu, "Correlation between bulk modulus of ternary intermetallic compounds and atomic properties of their constituent elements," *Intermetallics*, vol. 12, no. 1, pp. 103–109, 2004.

[43] C. Li and P. Wu, "Correlation of bulk modulus and the constituent element properties of binary intermetallic compounds," *Chemistry of Materials*, vol. 13, no. 12, pp. 4642–4648, 2001.

[44] D. Fan, W. Zhou, C. Liu et al., "Thermal equation of state of natural chromium spinel up to 26.8 GPa and 628 K," *Journal of Materials Science*, vol. 43, no. 16, pp. 5546–5550, 2008.